

# Effect of nanoparticles on the thermal stability of PMMA nanocomposites prepared by *in situ* bulk polymerization

Wantinee Viratyaporn · Richard L. Lehman

Received: 21 March 2010 / Accepted: 13 September 2010 / Published online: 9 October 2010  
© Akadémiai Kiadó, Budapest, Hungary 2010

**Abstract**  $\text{Al}_2\text{O}_3$  and  $\text{ZnO}$  filled poly(methyl methacrylate) nanocomposites were synthesized by free radical (bulk) polymerization. Efficient dispersion was achieved by predispersing the nanoparticles in propylene glycol methyl ether acetate (PGMEA) followed by ultrasonication of nanoparticles into the PMMA syrup. Thermal analysis confirms chemisorption between PGMEA and metal oxide particles. The addition of nanoparticle affects degradation mechanism and consequently improves thermal stability of PMMA. The reduction of polymer chain mobility and the tendency of nanoparticles to eliminate free radicals are the principal effects responsible for these enhancements.

**Keywords** Thermal analysis · Polymer nanocomposites · Alumina · Functionalization · Poly(methyl methacrylate)

## Introduction

Poly(methyl methacrylate), or PMMA, is an important thermoplastic for numerous uses and especially for optical applications due to excellent transparency in the visible region. Nevertheless, PMMA has limiting properties, particularly its low toughness and poor thermal stability. In the polymerization process the termination reaction of propagating chains can occur either through disproportionation or combination reactions depending on the stability of the propagating radical. The disproportion reaction yields two polymer chains, one with saturated chain ends and the second with unsaturated. The combination reaction, on the

other hand, results in one long polymer chain with head-to-head (H–H) configuration at the linkage. Both the unsaturated chain end and the head-to-head linkage are defects in the polymer chain that significantly affect the thermal stability of polymers [1–3].

Thermal degradation of PMMA has been extensively examined [1–7]. Kashiwagi et al. studied thermal degradation of PMMA polymerized by free radical polymerization at a heating rate of  $2\text{ }^\circ\text{C min}^{-1}$  [1]. Under nitrogen atmosphere, the thermal degradation of PMMA typically consists of three steps: scission initiated at head-to-head linkage ( $165\text{ }^\circ\text{C}$ ), scission initiated at unsaturated chain end ( $270\text{ }^\circ\text{C}$ ), and random scission of polymer main chain ( $360\text{ }^\circ\text{C}$ ). The instability of the H–H linkage is attributable to the close proximity of the bulky pendent groups creating higher localized free energy via steric hindrance as well as the inductive effect of the ester groups with respect to electron extraction. Consequently, the bond dissociation energy of this H–H linkage was found to be about  $84\text{ kJ mol}^{-1}$  less than that of C–C backbone bond [1]. The second weakest point is at the unsaturated end group and the scission at this point was proposed to occur at the C–C bond in the  $\beta$  position to the unsaturated vinylidene end group since the dissociation energy of the C–C bond in this position is approximately  $42\text{--}50\text{ kJ mol}^{-1}$  lower than the adjacent saturated C–C bond. This is known as the  $\beta$ -scission [1]. The last and the most stable bond is the C–C main chain bond which will decompose at the highest temperature. The breaking of the main chain will result in one primary radical and one tertiary radical followed by the  $\beta$ -scission that will depolymerize to MMA [4].

Details of each step of the thermal degradation of PMMA have been elucidated in comprehensive studies [2, 3, 6]. At a heating rate of  $20\text{ }^\circ\text{C min}^{-1}$ , head-to-head scission of PMMA appears around  $250\text{--}300\text{ }^\circ\text{C}$ , although scission

W. Viratyaporn · R. L. Lehman (✉)  
AMIPP Advanced Polymer Center, School of Engineering,  
The State University of New Jersey, Rutgers, Piscataway,  
NJ 08854-8065, USA  
e-mail: rlehman@rutgers.edu

frequency is reduced as polymer chain becomes larger. Such increase in chain length results from a large cage effect which leads to recombination of the degradation species. The degradation of unsaturated end groups was observed at around 180–200 and 290–300 °C and proposed to undergo the radical transfer mechanism. Finally, the main chain scission occurs around 350–400 °C. The homolytic degradation of the side chain appears to be more efficient in the degradation of PMMA, again due to cage effect dynamics.

The incorporation of nanoparticles into polymer systems has demonstrated the improvement in thermal stability of polymer [8–16]. A study of radical polymerization of the ZnO/PMMA system reported that the ZnO surface-induced chain termination, thus leading to less defect linkage elements (e.g., H–H) that would be created during polymerization of the neat PMMA [15]. Moreover, the effect of nanoparticles on increasing the thermal stability of polymeric materials was proposed through several mechanisms such as the barrier effect in which nanoparticles retard heat and mass transport necessary for the degradation process [9, 10]. Paramagnetic iron present in clay particles is key to a proposed radical trapping mechanism which enhances the thermal stability of the clay/polymer composites [11]. Furthermore, the thermal stability was also reported to be enhanced by the restriction of the polymer chain mobility in particle/polymer composites [13, 14].

In our study, we examined the effect of particle chemistry and size on the thermal stability of PMMA. Two types of particle chemistry were chosen, aluminum oxide ( $\text{Al}_2\text{O}_3$ ) and zinc oxide (ZnO). In the aluminum oxide part of the study, we investigated the effect of dry and pre-dispersed powders to assess the effect of the dispersing medium. In the case of zinc oxide nanoparticles, two particle sizes were selected and both were used as the pre-dispersed nanoparticles.

## Experimental

### Materials

Poly(methyl methacrylate) bead (Mw = 75,000, Polysciences, Inc., Warrington, PA) and stabilized methyl

methacrylate monomer, MMA (Acros Organics, Morris Plains, NJ), were obtained commercially. PMMA and MMA have densities of 1.19 and 0.93 g cm<sup>-3</sup>, respectively. Azobis isobutyronitrile (AIBN) initiator was purchased from Aldrich and used as received without recrystallization. Aluminum oxide ( $\text{Al}_2\text{O}_3$ ) and zinc oxide (ZnO) nanoparticles were obtained from Nanophase Technologies, Romeoville, IL, as either dry powder or dispersed in propylene glycol monomethyl ether acetate (PGMEA or PMA). Further details regarding the physical properties and form of the nanoparticles are given in Table 1.

### In situ polymerization of PMMA/nanocomposites

The MMA was purified by passing inhibited MMA through a column packed with aluminum oxide to remove the inhibitor by adsorption. Syrup was prepared by mixing 15 vol% of PMMA micro beads with 85 vol% purified MMA followed by magnetic stirring for 24 h at ambient. The oxide nanoparticles were dispersed in the syrup by first placing the weighed amount of particles in the bottom of a beaker and then adding the appropriate amount of syrup on top. Detailed quantities of the polymer nanocomposites are shown in Table 2. This mixture was sonicated for 20 min at 350 Watts, for a total energy application of 420 kJ. The 1 wt% of AIBN initiator was introduced to the mixture and stirred with a magnetic bar for 5 min. Subsequently, the mixture was put under a mechanical vacuum for 5 min. Sheet molds prepared from two glass plates sealed with window spacing tape was filled with the degassed mixture and placed into a water bath at 50 °C for 24 h to polymerize the composite and to develop initial strength. A final cure was conducted at 95 °C for 1 h.

### Thermal gravimetric analysis (TG)

Thermal stability of the composites was determined by thermal gravimetric analysis (TG) under flowing N<sub>2</sub> atmosphere (20 mL min<sup>-1</sup>) and a heating rate of 10 °C min<sup>-1</sup>. The test was performed on the TGA 7 from Perkin-Elmer. The PGMEA-stabilized nanoparticles were

**Table 1** Nanoparticles information

Trade name	Type	Quantity in PMA/vol%	$d^a/\text{nm}$	Morphology
NanoTek® Aluminum oxide, Dry powder	$\text{Al}_2\text{O}_3$	–	45	Sphere
NanoArc® R1130PMA	$\text{Al}_2\text{O}_3$	10.35	20	Sphere
NanoDur® X1130PMA	$\text{Al}_2\text{O}_3$	21.23	45	Sphere
NanoArc® Q1102PMA	ZnO	10.35	20	Elongated
NanoTek® ZH1102PMA	ZnO	10.35	35	Elongated

<sup>a</sup> Mean particle size

**Table 2** Composition information

Sample	Nanoparticle		PMMA/vol%	PMA/vol%
	Type	Vol%		
PMMA	—	—	100.00	—
PMMA/PGMEA-1	—	—	99	1
PMMA/PGMEA-3	—	—	97	3
PMMA/PGMEA-5	—	—	95	5
PMMA/PGMEA-7	—	—	93	7
PMMA/Dry-Al <sub>2</sub> O <sub>3</sub> _45	Dry-Al <sub>2</sub> O <sub>3</sub> (45 nm)	1.00	99.00	—
PMMA/FG-Al <sub>2</sub> O <sub>3</sub> _45	FG-Al <sub>2</sub> O <sub>3</sub> (45 nm)	0.99	95.34	3.67
PMMA/FG-ZnO_20	FG-ZnO (20 nm)	0.92	91.11	7.97
PMMA/FG-ZnO_35	FG-ZnO (35 nm)	0.92	91.11	7.97

measured as is without any previous drying process to avoid errors from the volatilization of PGMEA. The temperature range was 20–700 °C. For the polymer–inorganic nanocomposites, the sample was cut from the sheet and run at the temperature range of 25–600 °C.

#### Differential scanning calorimetry (DSC)

The glass transition of PMMA/particulate nanocomposites was characterized by modulated DSC (Q1000 from TA Instrument, Delaware). Samples of approximately 10 mg were cut from the polymerized sheet and sealed in aluminum pans. DSC runs, heat–cool–modulated heat, were conducted over the temperature range of 30–180 °C with the modulated heat of ±1.300 °C every 40 s. The system was purged with nitrogen gas at flow rate of 50 mL min<sup>-1</sup>.

## Results and discussions

### Pre-dispersed nanoparticles

Dispersion is a critically important parameter in nearly all types of composite materials. In nanocomposites, the high ratio of surface forces to inertial forces of the nanoscale particles tends to encourage aggregation and agglomeration. To minimize these issues in the present composites, the nanoparticles used in this study were pre-dispersed in propylene glycol methyl ether acetate (PGMEA or PMA) to stabilize the nanoparticles and to prevent them from agglomeration. The polar PGMEA molecules are anticipated to chemisorb with the hydroxyl groups on the metal oxide surface, thus maintaining dispersion principally by a steric hindrance mechanism. This chemisorption was supported by TG traces (Fig. 1) for various types of stabilized nanoparticles in which chemically bonded PGMEA is evolved at temperatures above ~140 °C.

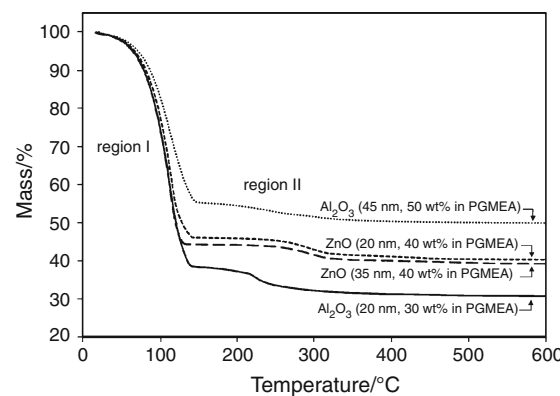


**Fig. 1** TG curve of various nanoparticles: region I is the reduction of the excess PGMEA and region II is the decomposition of the chemisorbed molecules

**Table 3** Mass percent of PGMEA on nanoparticle surface (Region II)

	20 nm	35 nm	45 nm
Aluminum oxide, Al <sub>2</sub> O <sub>3</sub>	3.3	—	2.0
Zinc oxide, ZnO	3.6	3.1	—

The mass loss curve contains two distinct regions, labeled as region I and II. Region I is associated with the loss of excess (i.e., non-bonded) PGMEA molecules while the chemisorbed molecules are more tightly bond and are not evolved until higher temperatures are reached, region II. Since the PGMEA is bonded to the nanoparticles, albeit via weak secondary bonds, we subsequently refer to the particles as functionalized and use the nomenclature FG-nanoparticles henceforth. An interesting aspect of this graph is the quantitative mass loss through Region II, which corresponds to the quantity of bonded PGMEA. These values are detailed in Table 3 ranging from 2 to 4% depending on the particle size and chemistry of the

nanoparticles. Naturally, the final mass of all specimens in the TG trace corresponded to the inorganic content of the dispersion as formulated and this value was used as a confirming check on the performance of the TG analysis.

The secondary bonding interaction between the PGMEA and the oxide particles was found to depend on the size of the particle and the specific oxide type. Smaller particles of both  $\text{Al}_2\text{O}_3$  and  $\text{ZnO}$  have adsorbed higher amounts of PGMEA, as expected from the higher surface area and as illustrated in the Figs. 1 and 2. Most interesting from this study, however, is the profile of the derivative mass loss curve that illustrates the temperature of maximum mass loss rate and the shape of the area under this curve, a behavior that is determined jointly by the particle size and oxide nature. Both aluminum oxide nanoparticles showed peak derivative loss rates in the temperature range 223–240 °C, whereas both zinc oxide nanoparticles showed the peak near 300 °C which may be a result of more tightly bound between the PGMEA and  $\text{ZnO}$  particle. A correlation of the area under the derivative mass loss curves with particle size shows that the integrated area is principally a function of the particle size with a secondary effect of oxide. Ionic potential is a determining factor for electron density at the metal oxide surfaces. The lower ionic potential ( $q/r$ ) of  $\text{ZnO}$  (~2.7) compared to  $\text{Al}_2\text{O}_3$  (~5.6) arises from the high proton concentration at the oxide surface and leads to increased interaction with both carbonyl and carboxylate ionic groups. This greater secondary bonding of  $\text{ZnO}$  particles is reflected in the insert in Fig. 2 that illustrates the greater area under the derivative curve for these particles after the effect of particle size is factored.

#### Behavior of neat PMMA

Neat poly(methyl methacrylate) is known to have poor thermal behavior. A study of thermal degradation temperature

of PMMA by TG showed that the polymer degrades in three steps at 180, 250, and 350 °C with a heating rate of 10 °C min<sup>-1</sup> [16]. The degradation mechanisms are given as the scission of H–H linkage, the scission of the vinylidene end group, and the random scission of polymer main chain, respectively. In our study, two degradation steps were observed in the neat PMMA, as shown in the Fig. 3. However, with careful investigation of the derivative curve, many overlapping peaks were detected in the temperature range 260–405 °C where the first part of the degradation (260–350 °C) was associated to scissions at the H–H linkage and the unsaturated end group and the second half (350–405 °C) was attributed by the degradation of polymer main chain. Additionally, PMMA polymerized in the presence of some oxygen will form occasional peroxide linkages [17]. In the presence of oxygen, the thermal degradation of PMMA is suppressed particularly at low temperature [1, 7]. The radical generated from head-to-head scission and unsaturated end group can react with oxygen molecules and form more stable species which subsequently improves the thermal stability of PMMA at low temperature. Correspondingly, in our study the PMMA specimens were polymerized in a sealed mold, but not in an oxygen-free environment, such that the ambient oxygen molecules are available to react with the propagating radical and form peroxide in the polymer chain. As a result, low temperature degradation is suppressed.

The net result of all these considerations is that the derivative mass loss curve of the neat PMMA (Fig. 3) peaks at 330 °C and is comprised of multiple contributions from the various decomposition mechanisms discussed above. Considerable uncertainty exists in the literature regarding the exact transitions generating each individual peak. For this reason, we do not provide specific mechanisms for the individual peaks, such as at 260, 330, 350, or 390 °C, but rather characterize the decomposition in terms of the overall range and temperature corresponding to the

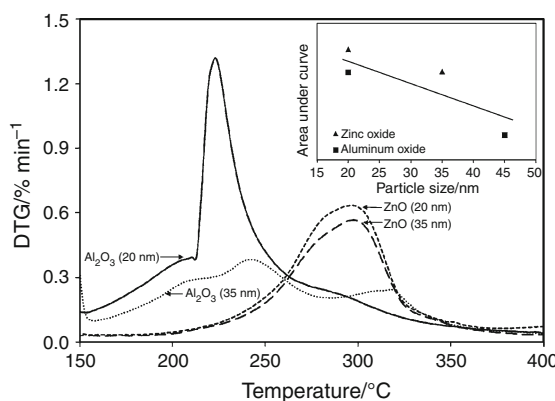


**Fig. 2** DTG curve of chemisorb molecules (region II) of various nanoparticles and the area under region II (inserted)

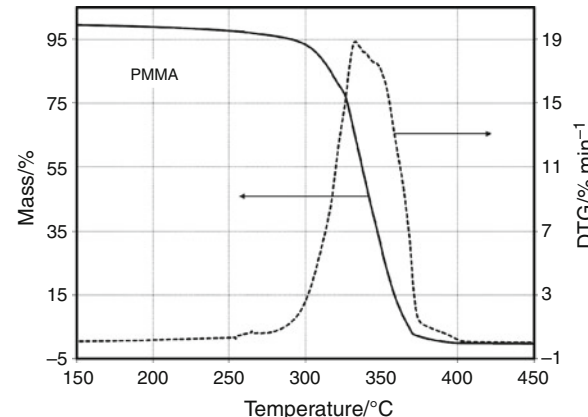


**Fig. 3** DTG and TG curves of neat PMMA

maximum rate, i.e., range = 260–405 °C and maximum = 350 °C.

### Polymer–inorganic nanocomposites

#### *PMMA/Aluminum oxide*

The thermal stability of PMMA is improved by the addition of alumina nanoparticles (Fig. 4). In the system containing pre-dispersed nanoparticles, mass loss commences very subtly near 145 °C (coincidentally the approximate boiling point of PGMEA), whereas when dry powders are used the measurable mass loss commences around 212 °C. The early mass loss associated with the PGMEA containing systems is a very small, but reproducible, effect and is not readily apparent in the figures, but was examined closely during data analysis. Comparing the decomposition of these alumina-filled composites with neat PMMA, the thermal stabilities of defect and main chain decompositions in alumina-filled composites are shifted toward lower and higher temperatures, respectively. At low temperatures the peak maximum is shifted from 330 °C (neat PMMA) to approximately 300 °C (alumina-filled composites). The random main chain scission, on the other hand, increases from ~350 °C (neat PMMA) to 375 °C (FG-Al<sub>2</sub>O<sub>3</sub>-filled) and 385 °C (dry-Al<sub>2</sub>O<sub>3</sub>-filled). The reduction in thermal stability at low temperature may result from oxygen absorption by the metal oxide surface [18] which reduces the amount of free oxygen in the alumina-filled composites and leads to fewer peroxide linkages in the composites, thus reducing the thermal stability at low temperature. An interesting subtlety of the low temperature region is that the dry alumina particles drive the low temperature decomposition to a slightly lower temperature than do the FG-Al<sub>2</sub>O<sub>3</sub> particles, but the amount of decomposition is less. Both of these effects are consistent with the peroxide-reduction mechanism given. The increase in thermal stability in the main chain scission region appears to result from several interactions between the polymer chain and the oxide particle surface, as described subsequently in this article.

#### *PMMA/Zinc oxide*

The zinc oxide composites demonstrated greater thermal stability than the alumina composites, i.e., the derivative peak maximum occurred at higher temperatures. Furthermore, the derivative mass loss curve exhibited just one principal peak as compared with the dual peaks observed for the alumina composites, with the caveat that other small artifacts exist on the derivative curve. Both the 20 and 35 nm zinc oxide composites displayed virtually the same

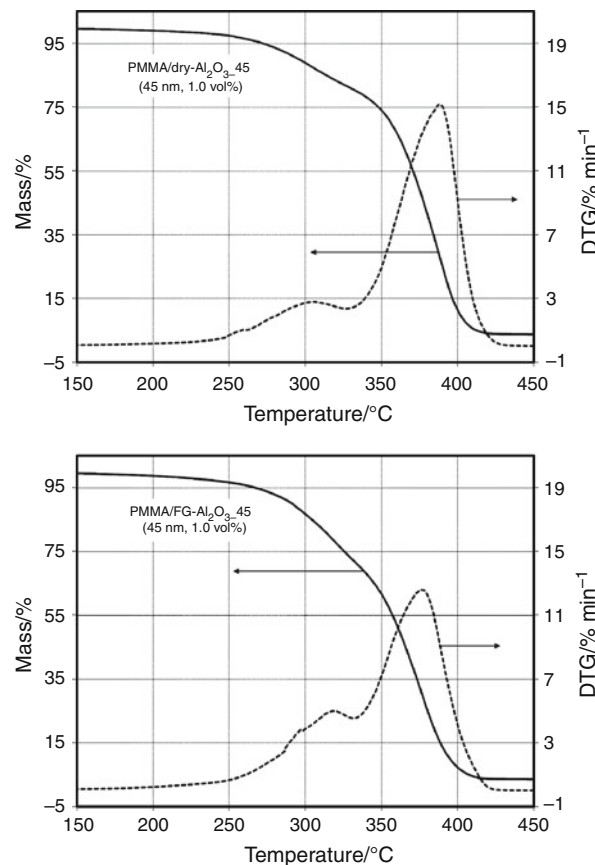


**Fig. 4** TG and DTG curves on the effect of aluminum oxide nanoparticles and small molecules of PGMEA on the thermal stability of PMMA

behavior with derivative curve peaks at ~390 °C. This reflects a substantial increase of nearly 50 °C in thermal stability over the neat polymer.

### Mechanisms

From the mass loss curves the degradation rate of polymer nanocomposites via chain defect site (H–H and vinylidene end group) initiation is decreased, particularly in the PMMA/FG-ZnO system. The vast bulk of the decomposition of PMMA in nanocomposites occurs as the main chain undergoes scission, which is shifted toward the higher temperature when nanoparticles are present. The effect is largest for the zinc oxide nanoparticle composites in which decomposition peaks (Fig. 5) occur at 392 and 389 °C for zinc oxide particles sizes of 20 and 35 nm, respectively. Aluminum oxide particles were somewhat less effective, although element type and particle size are partially confounded in this study, as evidenced by maximum degradation peaks at 388 and 375 °C, respectively for 45 nm alumina particles incorporated “dry” and “wet” respectively. The greater effectiveness of zinc oxide nanoparticles in improving the thermal

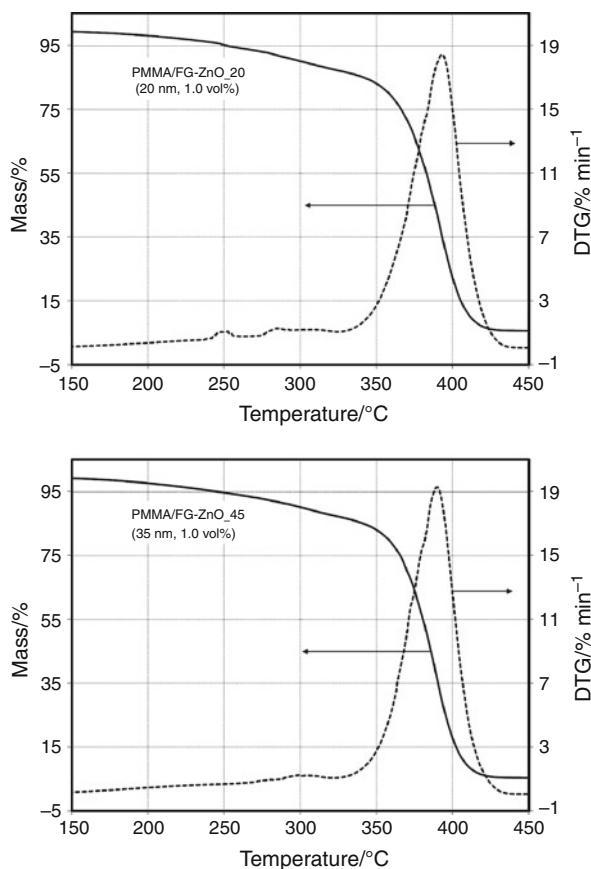


**Fig. 5** TG and DTG curve on the effect of zinc oxide nanoparticles on the thermal stability of PMMA

stability of PMMA seems to result from the higher surface proton density for zinc oxide ( $ZPC = 9.2$  for  $ZnO$  [19, 20] and 7.5 for  $Al_2O_3$  [21, 22]) compared to alumina as well as the smaller particle size of the zinc oxide.

Two mechanisms are commonly used to explain the increase in the thermal degradation temperature of the polymer nanocomposites. Both mechanisms involve interruption of the physical and/or chemical environment of the polymer. The first mechanism is comprised simply of steric hindrance of polymer chain motion that reduces thermally induced strain on the polymer backbone and also reduces the number of chain-scission-promoting encounters with neighboring moieties [14]. The second mechanism, which is not well documented in the literature, addresses the chemical inducing and inhibiting effects of nanoparticle oxide surfaces. The localization of charge arising from the carbonyl dipole and similar surface moieties may be effective in promoting bond scission, particularly as the charge destabilizes polymer units and promotes various scissions including the vinylidene decomposition discussed above. Countering this mechanism is the tendency for

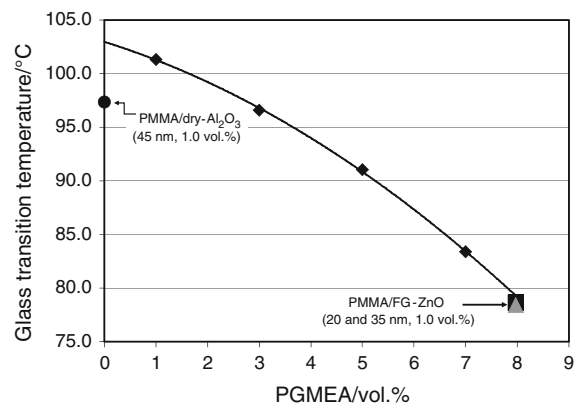


**Fig. 6** Glass transition temperatures of PMMA and PMMA nanocomposites

nano particles to act as defect getters during the fabrication [15] which reduces the concentration of H–H linkage and unsaturated end groups during polymer degradation [11], thus stabilizing the composite during subsequent heating.

In order to determine whether the improvement in thermal stability is caused by chain restriction, the glass transition temperature of the composites was examined, as shown in Fig. 6. Glass transition temperature ( $T_g$ ) is directly related to the polymer chain mobility. Thus, according to this concept, if nanoparticles are added to the polymer they will obstruct polymer chain motion and  $T_g$  will increase. However, there are data based on studies of thin polymer films and on certain nanocomposites that indicate a decrease in  $T_g$  as the film thickness (or the spacing between non-functionalized nanoparticles) decreases [23]. The thinking is that if the polymer is not constrained at its boundaries, as in a free film or in nanocomposites of non-functionalized particles, the structural relaxation process can continue to a more stabilized state corresponding to a lower  $T_g$ . In this study, we observed results that are more consistent with this latter model. Additions of dry, non-functionalized alumina nanoparticles to PMMA yielded a  $T_g$  of  $\sim 97$  °C, lower than the  $T_g$  of neat PMMA. On the other hand, when functionalized zinc oxide particles (PGMEA functionalized) were added to PMMA, the  $T_g$  did not change relative to the normalized value of 78 °C applicable to the result of PMMA plasticized with a corresponding quantity of PGMEA as shown in Fig. 6.

These data suggest that non-functionalized alumina particles slightly decrease the  $T_g$  of the composite and increase the chain mobility slightly by the “thin film” model noted above from the literature, whereas functionalized particles maintain the integrity of the polymer network and have little net effect on the structural relaxation of the polymer as measured by  $T_g$ .

## Summary

Polymer nanocomposites were prepared from PMMA and various alumina and zinc oxide nanocomposites with the aid, in most cases, of PGMEA as a functionalizing and dispersing agent. Initial studies addressed the degree of chemical interaction between the particles and the PGMEA. Significant chemisorption of PGMEA on the nanoparticle surface occurs via secondary bonding. PGMEA shows a greater affinity for the zinc particles due to higher surface proton concentrations, although the principal determinant overall was the greater surface area of smaller particles.

The thermal stability of the PMMA was improved by the addition of both the zinc oxide and aluminum oxide nanoparticles, although the greatest increase of about 45 °C was observed for composites prepared from 20 nm functionalized zinc oxide. H–H and unsaturated end-chain scission mechanisms contributed minimally to the overall breakdown of the composites. The vast majority of the decomposition occurred due to random main chain scission. The mechanism for this increased stability appears to arise from two mechanisms, steric restriction of chain motion and radical deactivation by nanoparticles.

**Acknowledgements** The study was kindly sponsored by AMIPP Advanced Polymer Center, Rutgers University. In addition, we would like to thank Dr. Hyun Jun Kim for his assistance in thermal analysis.

## References

- Kashiwagi T, Inaba A, Brown JE, Hatada K, Kitayama T, Masuda E. Effects of weak linkages on the thermal and oxidative degradation of poly(methyl methacrylates). *Macromolecules*. 1986;19:2160–8.
- Manring LE, Sogah DY, Cohen GM. Thermal degradation of poly(methyl methacrylate). 3. Polymer with head-to-head linkages. *Macromolecules*. 1989;22:4652–4.
- Manring LE. Thermal degradation of poly(methyl methacrylate). 2. Vinyl-terminated polymer. *Macromolecules*. 1989;22:2673–7.
- Kashiwagi T, Inaba A, Hamins A. Behavior of primary radicals during thermal degradation of poly(methyl methacrylate). *Polym Degrad Stab*. 1989;26:161–84.
- Manring LE. Thermal degradation of saturated poly(methyl methacrylate). *Macromolecules*. 1988;21:528–30.
- Manring LE. Thermal degradation of poly(methyl methacrylate). 4. Random side-group scission. *Macromolecules*. 1991;24:3304–9.
- Peterson JD, Vyazovkin S, Wight CA. Kinetic study of stabilizing effect of oxygen on thermal degradation of poly(methyl methacrylate). *J Phys Chem B*. 1999;103:8087–92.
- Tang E, Cheng G, Ma X. Preparation of nano-ZnO/PMMA composite particles via grafting of the copolymer onto the surface of zinc oxide nanoparticles. *Powder Technol*. 2006;161:209–14.
- Gilman JW, Jackson CL, Morgan AB, Richard Harris J. Flammability properties of polymer-layered-silicate nanocomposites. Polypropylene and polystyrene nanocomposites. *Chem Mater*. 2000;12:1866–73.
- Wang J, Du J, Zhu J, Wilkie CA. An XPS study of the thermal degradation and flame retardant mechanism of polystyrene-clay nanocomposites. *Polym Degrad Stab*. 2002;77:249–52.
- Zhu J, Uhl FM, Morgan AB, Wilkie CA. Studies on the mechanism by which the formation of nanocomposites enhances thermal stability. *Chem Mater*. 2001;13:4649–54.
- Wang H, Meng S, Xu P, Zhong W, Du Q. Effect of traces of inorganic content on thermal stability of poly(methyl methacrylate) nanocomposites. *Polym Eng Sci*. 2007;47:302–7.
- Li Y, Zhao B, Xie S, Zhang S. Synthesis and properties of poly(methyl methacrylate)/montmorillonite (PMMA/MMT) nanocomposites. *Polym Int*. 2003;52:892–8.
- Laachachia A, Cocheza M, Ferriola M, Lopez-Cuestab JM, Leroy E. Influence of TiO<sub>2</sub> and Fe<sub>2</sub>O<sub>3</sub> fillers on the thermal properties of poly(methyl methacrylate) (PMMA). *Mater Lett*. 2005;59:36–9.
- Demir MM, Memesa M, Castignolles P, Wegner G. PMMA/Zinc oxide nanocomposites prepared by in situ bulk polymerization. *Macromol Rapid Commun*. 2006;27:763–70.
- Dong C, Ni X. The photopolymerization and characterization of methyl methacrylate initiated by nanosized titanium dioxide. *J Macromol Sci A*. 2004;A41:547–63.
- Boven G, Oosterling MLCM, Challa G, Schouten AJ. Grafting kinetics of poly(methyl methacrylate) on microparticulate silica. *Polymer*. 1990;31:2377–83.
- Džunuzović E, Marinović-Cincović M, Vuković J, Jeremić K, Nedeljković JM. Thermal properties of PMMA/TiO<sub>2</sub> nanocomposites prepared by in situ bulk polymerization. *Polym Compos*. 2009;30:737–42.
- Fouad OA, Ismail AA, Zaki ZI, Mohamed RM. Zinc oxide thin films prepared by thermal evaporation deposition and its photocatalytic activity. *Appl Catal B*. 2006;62:144–9.
- Mrowetz M, Sell E. Photocatalytic degradation of formic and benzoic acids and hydrogen peroxide evolution in TiO<sub>2</sub> and ZnO water suspensions. *J Photochem Photobiol A*. 2006;180:15–22.
- Dominguez JM, Hernandez JL, Sandoval G. Surface and catalytic properties of Al<sub>2</sub>O<sub>3</sub>–ZrO<sub>2</sub> solid solutions prepared by sol–gel methods. *Appl Catal A*. 2000;197:119–30.
- Xing B. Natural organic material characteristics affect the environmental behavior of manufactured nanoparticles. Sweden: Stockholm; 2009.
- Schadler L (2003) Polymer-based and polymer-filled nanocomposites. Wiley: Nanocomposite Science and Technology; 2003. p. 77–153.